Research Square

Preprints are preliminary reports that have not undergone peer review.
They should not be considered conclusive, used to inform clinical practice,
or referenced by the media as validated information.

Development of Tissue Culture Techniques and Comparative Metabolomics for Echeveria laui Calli

Shuangbin Fu

shuangbinfu@gmail.com

Zhejiang Academy of Agricultural Sciences https://orcid.org/0000-0002-3894-2576

Zhen Ying

Zhejiang Academy of Agricultural Sciences

Chaoxiang Chen

Zhejiang Hongwei Testing Technology Co., Ltd.

Yanping Yang

Zhejiang Academy of Agricultural Sciences

Research Article

Keywords: Echeveria laui, regeneration, proliferation, morphology, metabolism

Posted Date: February 21st, 2025

DOI: https://doi.org/10.21203/rs.3.rs-6005140/v1

License: This work is licensed under a Creative Commons Attribution 4.0 International License.
Read Full License

Version of Record: A version of this preprint was published at Plant Cell, Tissue and Organ Culture (PCTOC) on September 11th, 2025. See the published version at https://doi.org/10.1007/s11240-025-03170-8.

Development of Tissue Culture Techniques and Comparative Metabolomics for *Echeveria laui* Calli

Shuangbin Fu[1,2], Zhen Ying[1,2], Chaoxiang Chen[3], Yanping Yang[1,2*]

[1*]Zhejiang Institute of Subtropical Crops, Jingshan, Wenzhou, 325005, Zhejiang, China.
[2]Innovation Center of Chinese Medical Crops, Zhejiang Academy of Agricultural Sciences, Shiqiao, Hangzhou, 310004, Zhejiang, China.
[3]Zhejiang Hongwei Testing Technology Co., Ltd., Xijing 2nd, Wenzhou, 325000, Zhejiang, China.

*Corresponding author(s). E-mail(s): yangyp@zaas.ac.cn;
Contributing authors: shuangbinfu@gmail.com; yingzhen0908@126.com;
1043028430@qq.com;

Abstract

In recent years, the market for succulent plants has experienced rapid growth. To increase the yield and value of *Echeveria laui*, a member of the succulent family, a tissue culture method was established in this study. The highest callus induction rate (26.7%) was achieved on Murashige and Skoog (MS) medium supplemented with 3 mg·L^{-1} 6-benzylaminopurine (6-BA), 1 mg·L^{-1} α-naphthaleneacetic acid (NAA), and 0.1 mg·L^{-1} thidiazuron (TDZ). The highest proliferation coefficient (4.26) was observed on medium containing 3 mg·L^{-1} 6-BA and 1 mg·L^{-1} NAA. Seedlings were regenerated when calli were cultured on MS or 1/2 MS medium without plant growth regulators (PGRs). During proliferation, three distinct types of calli were identified and analyzed using morphological observations and widely targeted metabolomics. Morphological analysis revealed that regenerable calli (GCs) presented numerous granular buds on their surface, and the cells were regular and complete, contributing to their regenerability. Metabolomic analysis revealed that the differentially accumulated metabolites (DAMs) were primarily amino acids and their derivatives, with dUMP identified as a biomarker for distinguishing among the three callus types. Additionally, changes in phytohormone levels were observed across the different callus types. These findings provide a

valuable reference for optimizing culture systems, minimizing undesirable tissue changes, and enhancing propagation efficiency.

Keywords: *Echeveria laui*, regeneration, proliferation, morphology, metabolism

1 Introduction

The global succulent plant industry is experiencing robust growth driven by key factors, such as the unique geometric shapes of these plants, which often form rosettes, and their ability to retain high levels of moisture. These characteristics make succulents ideal as landscape plants, capable of withstanding extreme conditions, and as low-maintenance potted plants suitable for indoor spaces with minimal watering requirements (Cabahug et al, 2018; Gezer, 2023).

In China, the popularity of succulents as ornamental plants has surged in recent years, with consumers particularly drawn to variegation mutants exhibiting unique color variations, commonly referred to as Jin. In Chinese horticulture, Jin describes a special growth form characterized by a distinct color or texture, often appearing along the edges of the leaves, setting them apart from normal plants. Succulents with Jin are highly sought after and command premium prices in the market. Consequently, businesses actively induce Jin by manipulating temperature, light, water, nutrition, and other environmental factors.

Echeveria laui (*E. laui*) is a highly popular succulent species in China that is prized for its striking, powdery, pale blue to pinkish rosette-shaped leaves. A company provided us with select varieties and entrusted us with their propagation through tissue culture methods while also expressing interest in inducing Jin using this technique.

In vitro regeneration studies of succulent plants have been conducted primarily through direct and indirect (callus) organogenesis, as well as somatic embryogenesis (Gezer, 2023). Indirect organogenesis has been successfully implemented in several succulent species, as reviewed by Bouzroud et al. (Bouzroud et al, 2022). For example, in *Cotyledon orbiculata*, callus formation was induced from leaf explants on MS medium containing 10 μM BA and 2.0 μM NAA, whereas the greatest number of shoots was produced on medium supplemented with a combination of 5 μM TDZ and 2.0 μM 6-BA. Regenerated shoots were successfully elongated when transferred to half-strength MS medium containing 10 μM indole-3-butyric acid (IBA) (Kumari et al, 2016). Similarly, the greatest level of callus induction was achieved when leaf explants were inoculated on MS medium supplemented with 1.0 mg·L^{-1} 6-BA and 0.1 mg·L^{-1} NAA, whereas the addition of 2.5 mg·L^{-1} TDZ to this induction medium was found to be optimal for callus proliferation. The maximum number of shoots was obtained when calli were cultured on MS medium supplemented with 1.0 mg·L^{-1} BA and 0.2 mg·L^{-1} 2,4-Dichlorophenoxyacetic acids (2,4-D) (Liu et al, 2017).

Using a similar approach, we induced callus by culturing the leaves of *E. laui*on MS medium supplemented with BA and TDZ. During callus proliferation, we observed the emergence of different types of calli on the same or different media. On the basis of their regenerative competence and morphology, the callus types were classified as

follows: GCs, characterized by their ability to regenerate shoots and by their surface covered with granular buds; moderately regenerable calli (MGCs), which lack buds, appear vitrified, and have a smooth texture; and nonregenerable calli (NGCs), which are unable to regenerate shoots and display a loose, grainy structure with no buds on the surface. The occurrence of NGCs, and especially the random appearance of MGCs, negatively impacted the efficiency of plant regeneration.

To analyze these phenomena, different metabolomic approaches have been employed in some plant species, such as tamarillo (Caeiro et al, 2023), Korean pine (Peng et al, 2022) and sugarcane (Mahmud et al, 2015), to study the metabolic changes between different types of calli. These studies focused on sets of metabolites or metabolic pathways or used a broader approach by employing analytic techniques such as mass spectrometry or nuclear magnetic resonance (NMR) associated with chemometric methods to assess the main metabolites of interest or infer metabolic pathways involved in the responses.The findings underscore vigorous metabolic activity, particularly in starch and sucrose metabolism, which is closely linked to cell division, tissue differentiation, and organ formation (Eveland and Jackson, 2012; Xue et al, 2022) and may play a crucial role in embryogenic callus development and maintenance (Wang et al, 2022).

In addition to the metabolites identified in the metabolic analysis, phytohormones (both endogenous and synthetic) are among the most critical factors influencing callus induction, proliferation, and regeneration in tissue culture for a wide range of plant species. Endogenous phytohormones, in particular, play pivotal roles in regulating various aspects of plant growth and development, and their levels and interactions can significantly determine the embryogenic potential of the callus. For example, in barley, calli exhibiting the highest regeneration rate of green shoots also contained the highest levels of indoleacetic acid (IAA), trans-zeatin (tZ), and cis-zeatin (cZ) (Hisano et al, 2016). Abscisic acid (ABA), at low concentrations, has been shown to be beneficial for maintaining embryogenic potential in Korean pine (Liang et al, 2022) and *Medicago truncatula* (Kepczyńska and Orłowska, 2021). Conversely, salicylic acid (SA) is generally considered a negative regulator of plant growth but has been reported to promote callus formation in *Hypericum perforatum* L. (Gadzovska et al, 2013).

In summary, metabolites within complex biological systems are crucial for understanding an organism's overall metabolic profile, and elucidating metabolic differences between tissues can guide the optimization of culture systems, minimize undesirable tissue changes, and enhance regeneration efficiency. Therefore, in this study, we introduce a method for regeneration of *E. laui* via indirect (callus) organogenesis using leaf explants. We then analyzed three types of calli that appeared during cultivation through histological observations and metabolomic analysis to identify differences in morphology and key metabolites, aiming to determine the most important metabolites that confer regenerable competence to the calli.

2 Materials and methods

2.1 Plant material and sterilization

The commercial *E. laui* variety 'Fen Hong Jia Ren Jin' was used as the plant material. Leaves were cut from the seedlings and washed with tap water and detergent to remove any dirt. The leaves were subsequently surface sterilized by immersion in 75% (v/v) alcohol for 1 min, followed by treatment with 0.1% (w/v) $HgCl_2$ for 8 min. After being rinsed four times with sterile distilled water, the leaf explants were transferred to a sterile surface and cut into 5×5 mm squares.

2.2 Callus induction

The prepared explants were cultured on MS medium supplemented with various types and concentrations of PGRs, along with 30 $g{\cdot}L^{-1}$ sucrose and 5 $g{\cdot}L^{-1}$ agar. Each culture bottle contained 5 explants, with each treatment consisting of 20 explants (4 bottles). Each treatment was repeated three times. The explants were subsequently incubated in a growth room at 25±1°C under a 16 h photoperiod.

2.3 Callus proliferation and shoot induction

Following initial proliferation on the same induction medium, callus was subdivided into approximately 2 g callus was cut into approximately 2 g pieces (weighed on a balance on a clean bench) and transferred to MS medium supplemented with various types and concentrations of PGRs, 30 $g{\cdot}L^{-1}$ sucrose, and 5 $g{\cdot}L^{-1}$ agar. Each culture bottle contained 5 callus explants, with each treatment consisting of 20 explants (4 bottles), and each treatment was repeated three times. The proliferation coefficient was calculated as the increase in weight divided by the initial weight before inoculation.

2.4 Regeneration and accumulation

The calli with shoots were transferred to different media supplemented with with various types and concentrations of PGRs, 30 $g{\cdot}L^{-1}$ sucrose and 5 $g{\cdot}L^{-1}$ agar. Each culture bottle contained 5 explants, with each treatment consisting of 20 explants (4 bottles), and this process was repeated three times. Regenerated plants were then transferred from the medium to plastic pots containing autoclaved succulent nutrient soil and grown under greenhouse conditions.

2.5 Metabolite extraction and HPLC-MS/MS analysis

Different callus tissues (100 mg) were individually ground with liquid nitrogen, and the homogenate was resuspended in prechilled 80% methanol and 0.1% formic acid by vortex. The samples were incubated on ice for 5 min and then centrifuged at 15,000 g and 4°C for 20 min. Some of the supernatant was diluted to obtain a final methanol concentration of 53% with liquid chromatography-mass spectrometry (LC-MS) grade water. The samples were subsequently transferred to a fresh Eppendorf tube (Eppendorf, Germany) and then centrifuged at 15,000 × g and 4°C for 20 min. Finally, the supernatant was injected into the LC-MS/MS system for analysis (Want

et al, 2013). LC-MS/MS analyses were performed using an ExionLC™ AD system (SCIEX) coupled with a QTRAP® 6500+ mass spectrometer (SCIEX) in Genedenovo (Guangzhou, China).

2.6 Differentially accumulated metabolite identification

The variable importance in projection (VIP) score of the PLS model was applied to rank the metabolites that were best distinguished between the two groups. The VIP threshold was set to 1. In addition, a t test was also used as a univariate analysis for screening differentially abundant metabolites. Metabolites with a T-test p value≤0.05, VIP≥1 or a |log2FC|≥1 were considered differentially accumulated metabolites between two groups.

2.7 Data analysis

The data in this study were analyzed using the R platform (R Core Team, 2024). Data visualizations were generated primarily via the ggplot2 R package (Wickham, 2016). PLS-DA was applied to the comparison groups via the R package ropls (Thévenot et al, 2015) and visualized via the mixOmics R package (Rohart et al, 2017). A Venn diagram was generated using the ggVennDiagram R package (Gao et al, 2024).

2.8 Histology

Calli were first examined under a stereomicroscope (SZ61, Olympus, Japan) to observe the surface.

Paraffin sectioning and dehydration: The paraffin sections were placed sequentially in xylene I (Sinopharm Chemical Reagent, China) and xylene II for 20 min each, absolute ethanol I and absolute ethanol II for 5 min each, and 75% ethanol (Sinopharm Chemical Reagent, China) for 5 min, followed by washing with tap water.

Toluidine blue staining: After the plant tissue sections were immersed in the staining solution for approximately 2-5 min, they were washed with water. Then, the samples were submerged in clean xylene for 5 min and sealed with neutral resin (Sinopharm Chemical Reagent, China).

Safranin O/fast green: The sections were placed in alizarin red staining solution for 1-2 h, rinsed lightly with tap water to remove excess stain, and then sequentially immersed in 50%, 70%, and 80% gradient alcohol for 3-8 s each. The sections were then transferred to Fast Green (AidishenBio, China) staining solution for 30-60 s, after which they were dehydrated via three changes of absolute ethanol. All the samples were observed under an orthogonal optical microscope (ECLIPSE E100, Nikon, Japan).

SEM

Fixed: Callus tissue areas not exceeding 3 mm^2 were cut, gently rinsed with PBS, and then quickly immersed in electron microscopy fixing fluid (AidishenBio, China) at room temperature for 2 h. The fixed samples were rinsed three times with 0.1 mol/L phosphate buffer (PB, pH=7.4, Sinopharm Chemical Reagent, China), and each rinse lasted 15 min. The samples were subsequently fixed in 1% osmium acid (Ted Pella Inc., USA) in 0.1 mol/L PB at room temperature in the dark for 1-2 h, followed by three additional rinses with 0.1 mol/L PB for 15 min each.

Dehydration: The tissues were sequentially immersed in ethanol solutions with concentrations of 30%, 50%, 70%, 80%, 90%, and 95% and twice in 100% ethanol for 15 min each, followed by immersion in isopentane for 15 min.

Drying: The samples were dried using a critical point dryer (K850, Quorum, UK).

Sample conductivity analysis: The dried samples were mounted onto a sample stage using double-sided conductive carbon tape and coated with gold using an ion sputtering instrument (MC1000, Hitachi, Japan) for approximately 30 seconds.

Finally, the samples were examined under a scanning electron microscope (SU8100, Hitachi, Japan).

3 Results

3.1 Callus induction

Despite a low contamination rate, callus formation was not observed on the majority of media tested, with most explants exhibiting browning (Fig. 1A). Specifically, no callus induction occurred on media supplemented with 6-BA, NAA, or combinations of these two PGRs alone. Callus formation was only observed on media containing TDZ, including: 1 $mg{\cdot}L^{-1}$ 6-BA + 0.1 $mg{\cdot}L^{-1}$ NAA + 0.1 $mg{\cdot}L^{-1}$ TDZ, 3 $mg{\cdot}L^{-1}$ 6-BA + 0.1 $mg{\cdot}L^{-1}$ NAA + 0.1 $mg{\cdot}L^{-1}$ TDZ, or 3 $mg{\cdot}L^{-1}$ 6-BA + 1 $mg{\cdot}L^{-1}$ NAA + 0.1 $mg{\cdot}L^{-1}$ TDZ (Table 1). Among these effective treatments, the highest callus induction rate (26.7%) was achieved on medium supplemented with 3 $mg{\cdot}L^{-1}$ 6-BA + 1 $mg{\cdot}L^{-1}$ NAA + 0.1 $mg{\cdot}L^{-1}$ TDZ, significantly higher than the other effective treatments. Additionally, on these effective media, the calli appeared to initiate shoot formation during the observation period (Fig. 1A).

Table 1 Effects of different media on callus induction

6-BA ($mg{\cdot}L^{-1}$)	NAA ($mg{\cdot}L^{-1}$)	TDZ ($mg{\cdot}L^{-1}$)	Callus induction rate (%)
0	0	0	0
0	1	0	0
1	0	0	0
1	0.1	0	0
1	0.1	0.1	8.0±4.0 b
1	1	0	0
3	0.1	0	0
3	0.1	0.1	13.3±4.6 b
3	1	0.1	26.7±4.6 a

Note: Different letters represent significant differences.

3.2 Callus proliferation and shoot induction

To optimize callus proliferation, we investigated the effects of 16 different media using a completely randomized design (Fig. 2A). In general, media with a higher 6-BA concentration relative to NAA, designated as “right-up” (P2, 3, 4, 7, 8, and 12), exhibited

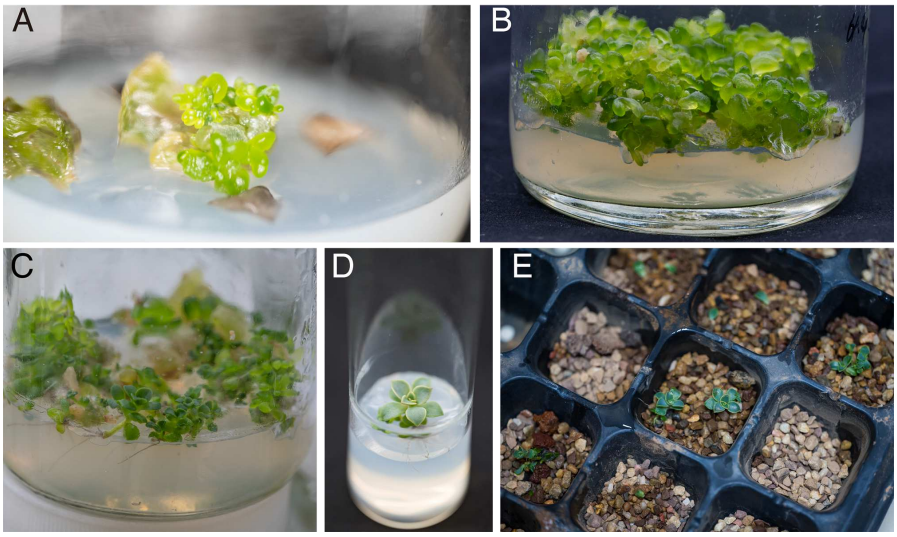


Fig. 1 *E. laui* callus induction, proliferation, regeneration and accumulation. **A**: Callus induction from explants cultured on MS medium supplemented with 3 mg·L^{-1} 6-BA + 1 mg·L^{-1} NAA + 0.1 mg·L^{-1} TDZ. **B**: Callus proliferation on medium medium supplemented with 3 mg·L^{-1} 6-BA + 1 mg·L^{-1} NAA. **C**: Seedlings regenerated on MS medium without PGRs D: Seedlings strengthened on the MS medium without PGRs. E: Seedlings acclimated in pots supplemented with nutrient soil.

higher proliferation coefficients compared to those with a lower 6-BA/NAA ratio, designated as "left-down" (P5, 9, 10, 13, 14, and 15), and those along the diagonal (P1, 6, 11, and 16). Medium P3 (3 mg·L^{-1} 6-BA and 1 mg·L^{-1} NAA) yielded the highest proliferation coefficient (4.26); however, this value was not significantly different from several other media, as indicated by shared lettering in Figure 2B. Notably, the calli displayed two distinct morphologies depending on the medium composition. Calli cultured on media with a high 6-BA/NAA ratio tended to form more shoot-like structures, whereas those cultured on media with a low 6-BA/NAA ratio appeared loose and granular. Except these, calli which lack buds, appear vitrifed, and have a smooth texture appeared randomly.

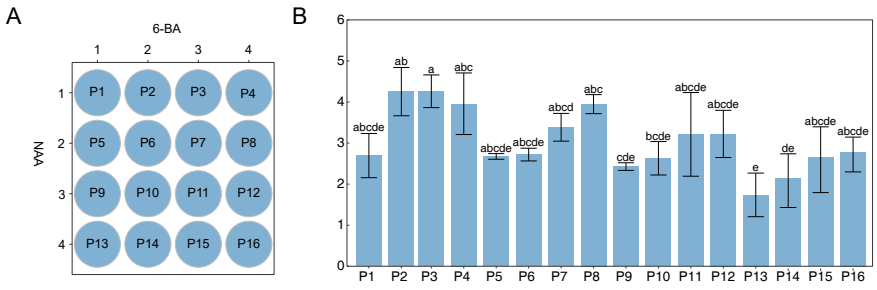


Fig. 2 Schematic of the media used and callus proliferation coefficients on different media. **A**: Experimental schematic for callus proliferation. **B**: Callus proliferation coefficient on different media. The same lowercase letters indicate no significant difference between treatments.

3.3 Regeneration and accumulation

High regeneration rates were observed across all tested media, with calli consistently producing seedlings. However, subtle differences in seedling development were noted. As detailed in Table 2, both full-strength MS and half-strength MS (1/2 MS) medium, when used without the addition of plant growth PGRs, supported particularly vigorous and robust seedling growth (Fig. 1C). Seedlings grown on these PGR-free media exhibited healthy development, characterized by well-developed roots and shoots. Following a strengthening period on the same respective media (MS or 1/2 MS without PGRs) to further enhance root and shoot development (Fig. 1D), the regenerated plantlets were successfully acclimated to *ex vitro* conditions by transplanting them into pots containing nutrient soil (Fig. 1E).

Table 2 Effects of different media on seedling regeneration

Medium	6-BA ($mg{\cdot}L^{-1}$)	NAA ($mg{\cdot}L^{-1}$)	Regeneration rate (%)	Description
MS	0	0	100	Rich, strength
MS	1	0.1	100	Median
MS	3	1	100	Median
1/2MS	0	0	100	Rich, strength
1/2MS	1	0.1	100	Median
1/2MS	3	1	100	Median

3.4 Histology and morphology

In addition to the above description, detailed morphological analysis further distinguished the three callus types. the morphology of the GCs was characterized by numerous granular buds covering their surface, these buds represent the initiation of organogenesis (Fig. 3A). In contrast, the surface of the MGCs appeared smooth and lacked buds, and the callus formed a solid block with a slightly hard texture and some vitrification (Fig. 3B). The NGCs, however, exhibited a loose and grainy structure with no buds on the surface (Fig. 3C). Histological observations following toluidine blue and safranin O/Fast Green staining revealed that NGCs and MGCs contained larger cells than did GCs. Additionally, the integrity and structural regularity of the GCs were superior to those of the NGCs and MGCs (Fig. 3D, E, F, G, H, I). The GCs showed densely packed cells with well-defined cell walls and organized cytoplasmic content (Fig. 3D, G), while NGCs and MGCs displayed loosely arranged cells with less distinct cell walls and evidence of cellular disorganization (Fig. 3E, F, H, I).

Scanning electron microscopy (SEM) further revealed these differences: the GCs presented fully developed, three-dimensional buds, further supporting their regenerative potential. The MGCs, however, exhibited numerous flaky tissues distributed across their surface (Fig. 3K), possibly representing disorganized cell divisions and the vitrification. In contrast, the surface of NGCs appeared stark and bare and was devoid of significant structural features (Fig. 3J, K, L).

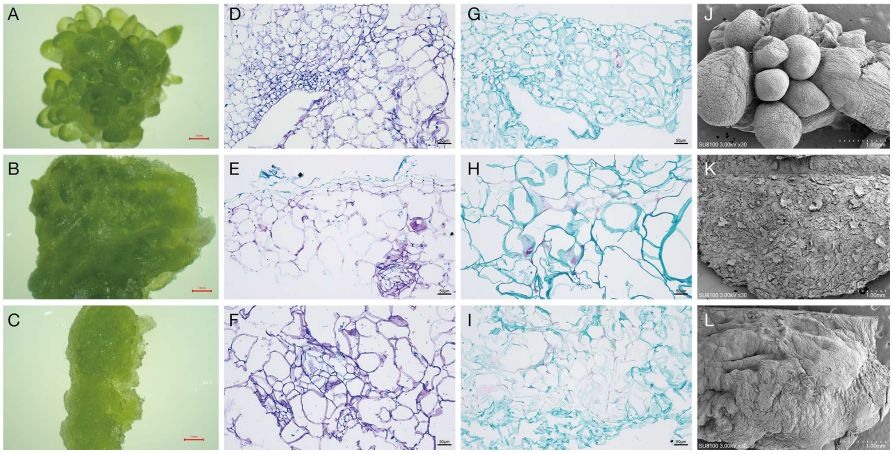


Fig. 3 Morphology and histology of different callus types. **A-C**: Morphology of different calli observed under a stereomicroscope; A to C, in order, are GCs, MGCs, and NGCs. Red arrows indicate shoots distributed on the surface of the GCs. **D-F**: Toluidine blue staining of different calli; D to F, in order, are GCs, MGCs, and NGCs. **G-I**: Safranin O/Fast Green staining of different calli; G to I, in order, are GCs, MGCs, and NGCs. **J-L**: Morphology of different calli observed via SEM; J to L, in order, are GCs, MGCs, and NGCs.

3.5 Sample consistency and overview of the metabolites

Partial least squares discriminant analysis (PLS-DA) clearly separated the GCs metabolite profile from the other two profiles, while there appeared to be some association between NGCs and MGCs (Fig. 4A). This overlap indicates that their metabolic profiles are more closely related to each other than either is to the GCs.

A total of 1008 metabolites were detected and classified into 20 groups, as shown in Fig. 4B. Among these, amino acids and their derivatives were the most abundant, with 186 identified metabolites, followed by flavonoids (134), lipids (115), carbohydrates and their derivatives (104), among others.

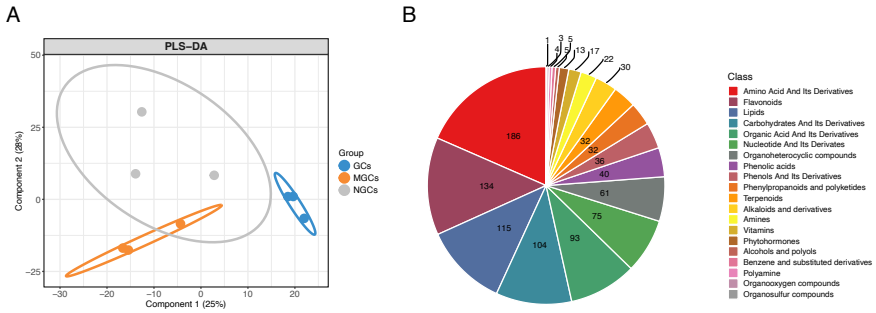


Fig. 4 Sample consistency and class of the metabolites. **A**: PLS-DA plot of the three groups. **B**: Class and number of detected metabolites.

3.6 DAM screening

On the basis of the P value, VIP or log2FC, 100 DAMs were selected from the GCs and NGCs comparison, 197 DAMs were selected from the GCs and MGCs comparison, and 56 DAMs were selected from the NGCs and MGCs comparison, which was the lowest number among the three comparisons (Fig. 5A, B, C). The top 5 metabolites are shown in Figure S1. Notably, amino acids and their derivatives were the most abundant DAMs in all three comparisons, dUMP was the only common DAM to all three comparisons (Fig. 5D).

Additionally, 4 types of phytohormones were selected, and the results revealed that the salicylic acid O-glucoside (SAG) and abscisic acid glucose ester (ABA-GE) levels increased in NGCs and MGCs, whereas the trans-zeatin N-glucoside (tZNG) and trans-zeatin riboside (tZR) levels decreased in both.

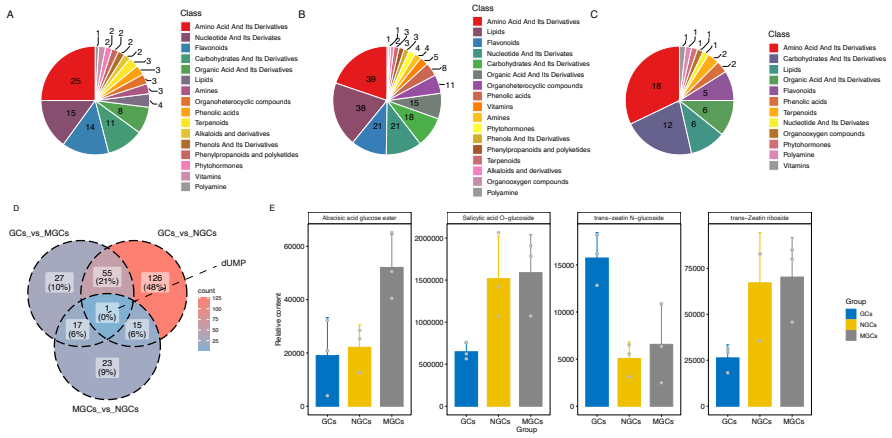


Fig. 5 Screening, classification, and distribution of DAMs in various comparisons. **A-C**: Classification and number of DAMs in the GCs_vs_NGCs, GCs_vs_MGCs, and NGCs_vs_MGCs comparisons. **D**: Venn diagram showing the overlap of DAMs across the three comparisons. **E**: Changes in the levels of four phytohormones in different callus tissues.

4 Discussion

4.1 Callus induction, proliferation and plant regeneration

In China, methods used to induce Jin in succulent plants involve controlling mainly temperature, light, and nutrient levels. While these conditions are also controllable *in vitro*, an additional advantage of tissue culture is the potential to utilize somaclonal variation that may arise during the process. Compared with spontaneous mutations occurring *in vivo*, somaclonal variations generated *in vitro* appear to occur more frequently (Yang et al, 2010). This approach has proven successful in developing new cultivars with enhanced traits, including improved abiotic stress tolerance and disease resistance, across various crop species such as sugarcane, barley, wheat, rice, tomato,

potato, mustard, and banana (review by Bhojwani and Razdan) (Bhojwani and Dantu, 2013). However, in our study, no such phenotypic variations were observed; nearly all *in vitro* regenerated seedlings exhibited a uniform green color, lacking the desirable Jin traits of the mother plant. Molecular analysis at later developmental stages is necessary to confirm the absence of underlying genetic or epigenetic variations. Future research could explore the incorporation of chemical mutagens or alternative physical treatments to potentially induce the desired Jin variations.

Although numerous studies and reviews have demonstrated that callus formation typically occurs on media supplemented with high levels of either auxins or cytokinins (CKs) during the initial stages (Pérez-Molphe-Balch et al, 2015; Bouzroud et al, 2022), our experiments achieved only low callus induction efficiency on media containing high 6-BA, despite successful sterilization. This low efficiency was likely due, at least in part, to the limited availability of starting material, which restricted the number of replicates. Notably, TDZ appeared to be the key factor influencing callus induction, which aligns with findings from the micropropagation system of *Haworthia turgida* Haw., where TDZ plays a critical role in promoting callus formation and proliferation (Liu et al, 2017).

To address the challenges with callus initiation, we implemented a completely randomized design to optimize callus proliferation by adjusting PGR concentrations. Our aim was to promote callus proliferation while minimizing or avoiding shoot regeneration. Although previous studies on adventitious shoot regeneration used media with high BA or TDZ (Amoo et al, 2009; Kumari et al, 2016), no seedlings appeared on our corresponding media. However, our results are consistent with findings on callus proliferation in *Haworthia turgida* Haw., where the highest growth rate was achieved on medium containing 2.5 $mg{\cdot}L^{-1}$ TDZ, 1.0 $mg{\cdot}L^{-1}$ BA, and 0.1 $mg{\cdot}L^{-1}$ NAA.

Considering both our callus induction results and previous studies, TDZ appears to be a highly effective PGR for callus proliferation. However, elevated TDZ concentrations have been linked to hyperhydricity (vitrification) in various plant species (Huetteman and Preece, 1993; Wu et al, 2021). In three endangered cacti species *Escobaria minima* (Baird) D. Hunt, *Mammillaria pectinifera* (Ruempler) F.A.C. Weber and *Pelecyphora aselliformis* Ehrenberg (Giusti et al, 2002), TDZ, while associated with abundant callus formation, also induced hyperhydricity of axillary shoots. While we did not specifically investigate the direct link between TDZ concentration and hyperhydricity in this study, further research is needed to determine the factors contributing to MGC formation, including the potential roles of TDZ and BA.

4.2 Histological observation

The numerous granular buds observed on the surface of GCs clearly indicate their regenerative capacity. In contrast, MGCs and NGCs lacked these buds, and their cells appeared larger and more irregular than those of GCs. These distinct cellular characteristics correlate with their respective regenerative abilities. Previous studies have shown that the formation of embryogenic cells is often associated with specific morphological changes (Fehér et al, 2003). Similar differences in cell morphology have also been reported in nonembryogenic calli of fingerroot ginger (*Boesenbergia rotunda*) (Ng et al, 2016) and sugarcane (Silveira et al, 2013).

4.3 Metabolomics

Among the three comparisons, amino acids and their derivatives emerged as the largest class of DAMs. This may be attributed to the higher amino acid requirements for cell differentiation and division, which are essential for plant regeneration. Specifically, the differences in the number of amino acids and their derivatives between GCs and MGCs/NGCs highlight the unique metabolic profile of GCs and the similarities between NGCs and MGCs. These amino acids are not uniformly elevated in specific tissues but instead appear scattered across different samples (Figure S2). Notably, GCs exhibited relatively high levels of arginine, a compound reported to play a major role in tissue culture proliferation and growth (Jain et al, 1995). Higher levels of arginine have also been observed in somatic embryos compared to nonembryogenic calli in *Silybum marianum* (Khan et al, 2015) and fingerroot ginger (Ng et al, 2016).

Following amino acids and their derivatives, the most prominent classes were carbohydrates and their derivatives, organic acids and their derivatives, nucleotides and their derivatives, flavonoids, and lipids. These metabolites play important roles in energy production, storage and transfer. Previous studies have shown that embryogenic calli present increased metabolic demands, particularly for energy, amino acids, and lipids, due to their strong differentiation ability, whereas nonembryogenic calli primarily support basic cell proliferation and lack differentiation potential. For example, flavonoids constitute the third-largest group of natural products and highly diverse secondary metabolites derived from polyphenols (Santos et al, 2017). In citrus, where no detectable accumulation of flavonoids was found in undifferentiated calli, flavonoids accumulate after embryonic morphological changes (Moriguchi et al, 1999). Other studies have shown that flavonoids produced during SE in milk thistle may stimulate differentiation and create a more favorable environment for embryogenesis (Khan et al, 2015).

Other examples include tamarillo (Caeiro et al, 2023), Korean pine (Peng et al, 2022), *Larixkaempferi* (Lamb.) Carr. (Wang et al, 2022), and sugarcane (Mahmud et al, 2015), where significant changes in carbohydrates were observed between embryogenic and nonembryogenic calli. Although the up- and downregulation of carbohydrate levels varied across species, these findings collectively suggest that such metabolic changes can serve as biochemical biomarkers for embryogenic competence.

Among the three comparisons, dUMP was the only common metabolite, with its relative content being the highest in GCs, followed by NGCs and MGCs. Therefore, the content of this metabolite can serve as a marker to distinguish the three types of calli. Given its biological function, dUMP plays a critical role in DNA synthesis, acting as a precursor for dTMP (Stasolla et al, 2003; Kafer et al, 2004). We infer that GCs undergo extensive cell division and proliferation, processes that require substantial DNA synthesis. Consequently, the elevated levels of dUMP highlight its importance for supporting active cell proliferation in GCs.

In plant tissue culture, PGRs such as 6-BA, TDZ and NAA play crucial roles in callus induction, proliferation, and regeneration. Similarly, endogenous phytohormones can significantly influence plant growth and development even at very low concentrations (Davies, 2004; Lam-Son Phan Tran and Pal, 2014). Therefore, in this study, it was necessary to analyze their roles, although the differences among the three types of

calli were subtle. As shown in Figure 5, four types of hormones were detected. Among them, ABA-GE is a metabolic form of the plant hormone ABA, whereas SAG is a derivative of the plant hormones SA. Previous studies have shown that these conjugates function primarily in the storage or transport of the corresponding hormones, ABA and SA, which are involved in the response to abiotic stress conditions (Hayat et al, 2007; Zhang, 2012). The observed higher levels (upregulation) of ABA-GE and in NGCs and MGCs compared to GCs suggest that these callus types may be experiencing or responding to different levels or types of stress, potentially influencing ABA and SA signaling. While the measurement of ABA-GE and SAG provides valuable information, direct quantification of free ABA and SA would offer a more comprehensive understanding of the hormonal dynamics in these callus types. Furthermore, the observed differences in tZNG and tZR levels between GCs and NGCs/MGCs suggest a shift in CK partitioning. The lower level of tZR in GCs aligns with previous reports indicating that decreased ZR and total CK content are associated with enhanced embryogenic potential (Liang et al, 2022) and are crucial for the long-term maintenance of thriving embryogenic calli (Wu et al, 2021).

However, the observed differences in endogenous phytohormone levels alone do not fully explain the distinct regenerative capacities of the three callus types. The exogenously applied PGRs (6-BA and NAA) in the culture media likely exert a more dominant influence on callus proliferation and differentiation. The specific ratios of 6-BA and NAA in the different media likely override the endogenous hormonal signals to a significant extent, influencing the observed morphologies and developmental pathways. Further investigation, including gene expression analysis of hormone biosynthesis and signaling pathways, is necessary to fully elucidate the complex interplay between endogenous phytohormones and exogenous PGRs in regulating callus development and regeneration in *E. laui*.

5 Conclusion

Throughout the tissue culture process, CKs (6-BA and TDZ) emerged as the most effective PGRs, influencing induction, proliferation, morphology, regenerability, and metabolite changes. Metabolomic analysis revealed numerous DAMs, with dUMP highlighted as a potential biomarker. These metabolites may partially explain the differences among the three types of calli and offer valuable insights for optimizing tissue culture conditions, minimizing undesirable tissue changes. This can be achieved through targeted adjustments (PGR ratios, nutrient supplementation). However, metabolism alone cannot fully explain the functional mechanisms of the numerous DAMs among the three callus types and their underlying crosstalk. By integrating other omics data and adjusting the medium components, more questions may be answered.

Supplementary information. Supplementary Figure S1 and S2.

Acknowledgements. We appreciate the materials provided by Mr. Chaoxiang Chen.

Declarations

- Funding
  Project of Zhejiang Academy of Agricultural Sciences : 2024LY27FX05.
- Conflict of interest/Competing interest
  Not applicable.
- Ethics approval and consent to participate
  Not applicable.
- Author contribution
  S.F. and Z.Y.: data curation, investigation, methodology, and writing-original draft; C.C.: resources; Y.Y.: supervision and writing-review and editing. All authors have read and agreed to the published version of the manuscript.

References

Amoo SO, Finnie JF, Van Staden J (2009) In vitro propagation of Huernia hystrix: An endangered medicinal and ornamental succulent. Plant Cell Tissue Organ Cult 96(3):273–278. https://doi.org/10.1007/s11240-008-9484-8

Bhojwani SS, Dantu PK (2013) Somaclonal Variation, Springer India, India, pp 141–154. https://doi.org/10.1007/978-81-322-1026-9_12

Bouzroud S, El Maaiden E, Sobeh M, et al (2022) Micropropagation of *opuntia* and other cacti species through axillary shoot proliferation: a comprehensive review. Front Plant Sci 13. https://doi.org/10.3389/fpls.2022.926653

Cabahug RAM, Nam SY, Lim KB, et al (2018) Propagation techniques for ornamental succulents. Flower Research Journal 26(3):90–101. https://doi.org/10.11623/frj.2018.26.3.02

Caeiro A, Jarak I, Correia S, et al (2023) Primary metabolite screening shows significant differences between embryogenic and non-embryogenic callus of Tamarillo (*solanum betaceum* Cav.). Plants 12(15):2869. https://doi.org/10.3390/plants12152869

Davies PJ (2004) Plant hormones: biosynthesis, signal transduction, action!, 3rd ed. Kluwer Academic, Dordrecht

Eveland AL, Jackson DP (2012) Sugars, signalling, and plant development. J Exp Bot 63(9):3367–3377. https://doi.org/10.1093/jxb/err379

Fehér A, Pasternak TP, Dudits D (2003) Transition of somatic plant cells to an embryogenic state. Plant Cell Tissue Organ Cult 74(3):201–228. https://doi.org/10.1023/A:1024033216561

Gadzovska S, Maury S, Delaunay A, et al (2013) The influence of salicylic acid elicitation of shoots, callus, and cell suspension cultures on production of naphtodianthrones and phenylpropanoids in *hypericum perforatum* L. Plant Cell Tissue Organ Cult 113(1):25–39. https://doi.org/10.1007/s11240-012-0248-0

Gao CH, Chen C, Akyol T, et al (2024) ggVennDiagram: Intuitive Venn diagram software extended. iMeta 3(1):e177. https://doi.org/10.1002/imt2.177

Gezer APDR (2023) Tissue culture of ornamental succulent plants. Advances Plant Research p 107

Giusti P, Vitti D, Fiocchetti F, et al (2002) In vitro propagation of three endangered cactus species. Sci Hortic 95(4):319–332. https://doi.org/10.1016/S0304-4238(02)00031-6

Hayat S, Ali B, Ahmad A (2007) Salicylic acid: biosynthesis, metabolism and physiological role in plants. Salicylic acid: A plant hormone pp 1–14

Hisano H, Matsuura T, Mori IC, et al (2016) Endogenous hormone levels affect the regeneration ability of callus derived from different organs in barley. Plant Physiol Biochem 99:66–72. https://doi.org/10.1016/j.plaphy.2015.12.005

Huetteman CA, Preece JE (1993) Thidiazuron: A potent cytokinin for woody plant tissue culture. Plant Cell Tissue Organ Cult 33(2):105–119. https://doi.org/10.1007/BF01983223

Jain SM, Gupta PK, Newton RJ (eds) (1995) Somatic Embryogenesis in Woody Plants, Forestry Sciences, vol 44–46. Springer Netherlands, Dordrecht, https://doi.org/10.1007/978-94-011-0491-3

Kafer C, Zhou L, Santoso D, et al (2004) Regulation of pyrimidine metabolism in plants. Front Biosci 9(2):1611–1625. https://doi.org/10.2741/1349

Kepczyńska E, Orłowska A (2021) Profiles of endogenous ABA, bioactive GAs, IAA and their metabolites in medicago truncatula gaertn. non-embryogenic and embryogenic tissues during induction phase in relation to somatic embryo formation. Planta 253(3):67. https://doi.org/10.1007/s00425-021-03582-8

Khan MA, Abbasi BH, Ali H, et al (2015) Temporal variations in metabolite profiles at different growth phases during somatic embryogenesis of *silybum marianum* L. Plant Cell Tissue Organ Cult 120(1):127–139. https://doi.org/10.1007/s11240-014-0587-0

Kumari A, Baskaran P, Van Staden J (2016) In vitro propagation and antibacterial activity in Cotyledon *orbiculata*: a valuable medicinal plant. Plant Cell Tissue Organ Cult 124(1):97–104. https://doi.org/10.1007/s11240-015-0878-0

Lam-Son Phan Tran, Pal S (2014) Phytohormones: a window to metabolism, signaling and biotechnological applications. Springer, New York

Liang Y, Xu X, Shen H, et al (2022) Morphological and endogenous phytohormone changes during long-term embryogenic cultures in Korean pine. Plant Cell Tissue Organ Cult 151(2):253–264. https://doi.org/10.1007/s11240-022-02348-8

Liu B, Fang H, Meng C, et al (2017) Establishment of a rapid and efficient micropropagation system for succulent plant *haworthia turgida* Haw. Hortscience 52(9):1278–1282. https://doi.org/10.21273/HORTSCI12056-17

Mahmud I, Shrestha B, Boroujerdi A, et al (2015) NMR-based metabolomics profile comparisons to distinguish between embryogenic and non-embryogenic callus tissue of sugarcane at the biochemical level. In Vitro Cell Dev Biol-Plant 51(3):340–349. https://doi.org/10.1007/s11627-015-9687-8

Moriguchi T, Kita M, Tomono Y, et al (1999) One type of chalcone synthase gene expressed during embryogenesis regulates the flavonoid accumulation in citrus cell cultures. Plant Cell Physiol 40(6):651–655. https://doi.org/10.1093/oxfordjournals.pcp.a029589

Ng TLM, Karim R, Tan YS, et al (2016) Amino acid and secondary metabolite production in embryogenic and non-embryogenic callus of Fingerroot Ginger (*boesenbergia rotunda*). PLoS One 11(6):e0156714. https://doi.org/10.1371/journal.pone.0156714

Peng C, Gao F, Tretyakova IN, et al (2022) Transcriptomic and metabolomic analysis of Korean pine cell lines with different somatic embryogenic potential. Int J Mol Sci 23(21):13301. https://doi.org/10.3390/ijms232113301

Pérez-Molphe-Balch E, Santos-Díaz MdS, Ramírez-Malagón R, et al (2015) Tissue culture of ornamental cacti. Sci Agric 72:540–561. https://doi.org/10.1590/0103-9016-2015-0012

R Core Team (2024) R: a language and environment for statistical computing. Vienna, Austria

Rohart F, Gautier B, Singh A, et al (2017) mixOmics: An R package for 'omics feature selection and multiple data integration. PLoS Comput Biol 13(11):e1005752. https://doi.org/10.1371/journal.pcbi.1005752

Santos EL, Maia BHLS, Ferriani AP, et al (2017) Flavonoids: Classification, biosynthesis and chemical ecology. In: Justino GC (ed) Flavonoids-From Biosynthesis to Human Health. InTech, https://doi.org/10.5772/67861

Silveira V, de Vita AM, Macedo AF, et al (2013) Morphological and polyamine content changes in embryogenic and non-embryogenic callus of sugarcane. Plant Cell Tissue Organ Cult 114(3):351–364. https://doi.org/10.1007/s11240-013-0330-2

Stasolla C, Katahira R, Thorpe TA, et al (2003) Purine and pyrimidine nucleotide metabolism in higher plants. J Plant Physiol 160(11):1271–1295. https://doi.org/10.1078/0176-1617-01169

Thévenot EA, Roux A, Xu Y, et al (2015) Analysis of the human adult urinary metabolome variations with age, body mass index, and gender by implementing a comprehensive workflow for univariate and opls statistical analyses. J Proteome Res 14(8):3322–3335. https://doi.org/10.1021/acs.jproteome.5b00354

Wang J, Zhang L, Qi L, et al (2022) Integrated transcriptomic and metabolic analyses provide insights into the maintenance of embryogenic potential and the biosynthesis of phenolic acids and flavonoids involving transcription factors in *larix kaempferi* (lamb.) carr. Front Plant Sci 13. https://doi.org/10.3389/fpls.2022.1056930

Want EJ, Masson P, Michopoulos F, et al (2013) Global metabolic profiling of animal and human tissues via UPLC-MS. Nat Protoc 8(1):17–32. https://doi.org/10.1038/nprot.2012.135

Wickham H (2016) Ggplot2: elegant graphics for data analysis, Springer-Verlag, New York

Wu G, Wei X, Wang X, et al (2021) Changes in biochemistry and histochemical characteristics during somatic embryogenesis in *ormosia henryi* prain. Plant Cell Tissue Organ Cult 144(3):505–517. https://doi.org/10.1007/s11240-020-01973-5

Xue W, Liu N, Zhang T, et al (2022) Substance metabolism, IAA and CTK signaling pathways regulating the origin of embryogenic callus during dedifferentiation and redifferentiation of cucumber cotyledon nodes. Sci Hortic 293:110680. https://doi.org/10.1016/j.scienta.2021.110680

Yang WR, Zhang QX, Pan H, et al (2010) In vitro regeneration of lilium tsingtauense gilg. and analysis of genetic variability in micropropagated plants using rapd and ISSR techniques. Propagation of Ornamental Plants 10

Zhang Y (2012) Ascorbic acid in plants: biosynthesis, regulation and enhancement. Spring, New York

Supplementary Files

This is a list of supplementary files associated with this preprint. Click to download.

- FigureS1.pdf
- FigureS2.pdf